The Co–Al distances determined by Mrs Douglas vary somewhat about the average value discussed above. The variations might be attributed either to differences in bond numbers or to differences in the amount of d character of the cobalt orbitals. Their distribution in the crystal (especially the 180° angle between the strongest bonds) indicates that the second rather than the first effect is mainly involved. The smallest observed distance, 2·375 A., would result from a 2/3 bond with the cobalt bond orbital having 60% d character. The possibility of unequal distribution of d character among the bond orbitals permits a variety of behavior of the transition elements that is not shown by elements such as aluminum.

Additional experimental evidence about the electronic structure proposed here for Co_2Al_9 could be obtained by study of the magnetic properties of the substances. The above theory requires that the magnetic moment of cobalt in Co_2Al_9 be greater than in the elementary substance, whereas the theory of Raynor & Waldron requires that it be less.

References

Douglas, A. M. B. (1950). *Acta Cryst.* **3**, 19.
Pauling, L. (1947). *J. Amer. Chem. Soc.* **69**, 542.
Pauling, L. (1949). *Proc. Roy. Soc.* A, **196**, 343.
Raynor, G. E. & Waldron, D. M. B: (1949). *Phil. Mag.* **40**, 198.

Acta Cryst. (1951). **4**, 140

The Crystal Structure of α-Monoclinic Selenium*

By Robinson D. Burbank†

Laboratory for Insulation Research, Massachusetts Institute of Technology, Cambridge, Massachusetts, U.S.A.

(*Received* 29 *June* 1950)

The crystal structure of α-monoclinic selenium has been determined by the application of the Harker–Kasper phase inequalities and two-dimensional Fourier syntheses. The α-selenium molecule is an eight-membered, puckered ring similar to the rhombic sulfur molecule. It conforms, within the limit of experimental error, to the non-crystallographic point-group symmetry $\overline{8}2m$; the covalent bond distance is 2·34 ± 0·02 A., and the covalent bond angle is 105·3 ± 2·3°. Certain abnormally short packing distances are observed which are discussed in terms of the metallic character believed to be present in the intermolecular bonding of hexagonal selenium.

Introduction

Selenium exhibits a polymorphism comparable with that of sulfur in complexity. The familiar selenium of commerce is vitreous and can readily be converted into three crystalline polymorphs. A solution of vitreous selenium in carbon disulfide will yield two red, monoclinic varieties designated α and β respectively. Very slow cooling of vitreous selenium which has been heated to a fluid state will produce gray, hexagonal selenium, commonly called metallic selenium.

The relations that exist between the various modifications are known only in a qualitative way. Metallic selenium is the stable form at all temperatures up to the melting point (217° C.), and is obtained from any of the other forms on heating. There is no reverse transformation from the metallic form into any other form below 217° C., hence there is no real transition point in the physical-property curves of selenium.

It appeared desirable to investigate the crystal structures of both α- and β-selenium. The polymorphism of the element is confusing without a knowledge of the underlying atomic arrangement. The polymorphic transitions in sulfur are even more involved, and knowledge of crystal structures in the selenium system may benefit study of the sulfur system because of the several types of sulfur–selenium mixed crystals that are formed (Muthmann, 1890; Halla & Bosch, 1930). Von Hippel (1948) has discussed the progressive change in structure and conductivity for the known structures in the sequence oxygen, sulfur, selenium, tellurium, and polonium in terms of resonance between molecular and ionic structures, making use of Pauling's ideas on the metallic bond (Pauling, 1947). The structures of monoclinic selenium add more experimental data to be tested by this point of view.

The present paper, which presents the complete structure determination of α-selenium, is part of a program of this laboratory which it is hoped will clarify the existing gaps in the knowledge of the crystal chemistry of the element selenium.

Experimental procedure

High-purity selenium* was completely converted to the vitreous form by heating to a fluid state and

---

* Sponsored by the ONR, the Army Signal Corps, and the Air Force under ONR Contract N5ori–07801. From a thesis submitted in partial fulfillment of the requirements for the degree of Doctor of Philosophy in Inorganic Chemistry at the Massachusetts Institute of Technology.

† Present address: Carbide and Carbon Chemicals Division, K-25 Plant, Oak Ridge, Tennessee, U.S.A.

* Furnished by the American Smelting and Refining Company, New York, N.Y.

quenching in cold water. After air-drying and grinding to a fine powder the vitreous selenium was extracted in a Soxhlet apparatus with carbon disulfide until a saturated solution of a deep orange color was formed. Crystals of α-selenium were obtained by slowly evaporating the solution at room temperature for 72 hr., the volume of the solution decreasing about 10%. The crystal habit was highly modified and quite similar to that originally described by Mitscherlich (1856) with pyramidal forms most prominent.

Crystals less than 0·1 mm. in every dimension were chosen for X-ray examination to minimize serious absorption errors (μ for Mo $K\alpha$ radiation is 330 cm.$^{-1}$). The crystals were oriented with a precession camera (Buerger, 1944) and all unit-cell measurements were made with this instrument using Mo $K\alpha$ radiation, $\lambda = 0{\cdot}7107$ A. The results are as follows:

$$a = 9{\cdot}05 \pm 0{\cdot}01, \quad b = 9{\cdot}07 \pm 0{\cdot}01, \quad c = 11{\cdot}61 \pm 0{\cdot}01 \text{ A.},$$
$$\beta = 90^\circ\, 46' \pm 5'.$$
Space group $P2_1/n$.

The cell constants are in substantial agreement with the earlier measurements of Klug (1934). However, the space group $P2_1/n$ does not agree with the earlier work which reported it to be either $P2_1$ or $P2_1/m$. Precession camera photographs recorded 88 $h0l$ reflections with $h+l$ even, while 57 possible reflections with $h+l$ even were too weak to be detected. Out of some 145 reflections with $h+l$ odd, all of which would be possible for space group $P2_1$ or $P2_1/m$, not one was observed.

Intensity data were recorded with the precession camera using Mo $K\alpha$ radiation, and with the Weissenberg camera using Cu $K\alpha$ radiation. Multiple exposures were used with the precession method and multiple films with the Weissenberg technique. Intensities were estimated by visual comparison with a calibrated scale. The crystal habit was sufficiently complicated so that no attempt was made to calculate absorption corrections. The Lorentz and polarization factors were evaluated graphically, following the method of Evans for the precession camera (Evans, Tilden & Adams, 1949) and of Cochran (1948) for the Weissenberg camera. The observed structure factors are estimated to be in error by about ±15 percent.

Trial-and-error analysis

Warren & Burwell (1935) showed that 8-membered rings exist in the structure of rhombic sulfur. Muthmann (1890) observed that rhombic sulfur forms mixed crystals with up to 35 atomic percent of selenium. Halla & Bosch (1930) confirmed this with an X-ray examination of rhombic mixed crystals. The unit cell of α-selenium contains 32 atoms. Thus it seemed probable that α-selenium would contain four 8-membered ring molecules per unit cell, with a bond distance of 2·34 A. and a bond angle of 105° such as occurs in metallic selenium (Bradley, 1924). The type of molecule under consideration does not have a center of symmetry and would be located in the fourfold general positions of $P2_1/n$:

$$x, y, z; \quad \tfrac{1}{2}+x, \tfrac{1}{2}-y, \tfrac{1}{2}+z;$$
$$\bar{x}, \bar{y}, \bar{z}; \quad \tfrac{1}{2}-x, \tfrac{1}{2}+y, \tfrac{1}{2}-z.$$

Three strong $h0l$ reflections, 400, $\bar{5}03$ and $\bar{1}03$, and their higher orders, were observed to decrease in intensity in a regular manner with increase of $(\sin\theta)/\lambda$ and were thought to be somewhat near their maximum possible values. If it is required that these three sets of planes mutually intersect with no intersections occurring at symmetry centers, then the eight possible phase combinations will reduce to only two possibilities: 400 −, $\bar{5}03$ +, $\bar{1}03$ − and 400 −, $\bar{5}03$ −, $\bar{1}03$ +. These are equivalent since the origin of one set is related to the origin of the other by a translation of $\tfrac{1}{2}$, 0, 0 or 0, 0, $\tfrac{1}{2}$. Using the planes 400 −, $\bar{5}03$ +, and $\bar{1}03$ − a molecular orientation was sought which would place all the atoms near them. With the plane of the molecules parallel to the $\bar{1}03$ plane this objective seemed to be attained. Rough packing models seemed to be compatible with such an arrangement and structure-factor calculations were started using Bragg & Lipson charts. After a dozen trials the 70 lowest-order $h0l$ reflections gave a rough measure of agreement. The co-ordinates obtained at this point are illustrated in the left-hand cell of Fig. 3 and were interpreted, as in this diagram, in terms of a distorted 8-membered ring molecule which did not possess the high symmetry of the rhombic sulfur molecule.

An attempt was then made to confirm the preceding results by considering the $0kl$ reflections before proceeding further with the $h0l$ data. It finally became apparent that no reasonable correlation could be obtained using the parameters deduced from the $h0l$ reflections. Other conventional approaches did not appear promising after preliminary surveys and were abandoned.

Analysis by the Harker–Kasper phase inequalities

To apply the phase inequalities (Harker & Kasper, 1947, 1948) the experimental structure factors must first be placed on an absolute scale. Let F'_{hkl} represent a structure factor on a relative scale, and F_{hkl} represent the same structure factor on an absolute scale. Define a conversion factor K by the relation

$$|F'_{hkl}|^2 = K\,|F_{hkl}|^2.$$

Then K can be computed according to the expression (Harker, 1948)

$$K = \left(\overline{\frac{|F'_{hkl}|^2}{\sum_{j=1}^{n} f_j^2}}\right), \tag{1}$$

where the square of the numerical value of each structure factor on the relative scale is divided by the sum of the squares of the atomic scattering factors in the unit cell. Then an arithmetic average is taken over all the reflections used.

The atomic scattering factor used for selenium was obtained by averaging the Thomas–Fermi values with the Pauling–Sherman values. Some 200 *h0l* and *0kl* reflections were used in calculating the absolute scale which later proved to be about 13% lower than the scale calculated from the completed structure.

The structure factors on an absolute scale were converted to unitary structure amplitudes, U_{hkl}, by dividing by the sum of the atomic scattering factors in the unit cell.

Gillis (1948) has given a detailed example of the application of the phase inequalities, using the data for oxalic acid dihydrate, which is directly applicable to the present problem. The inequalities which are of paramount importance are, in Gillis's notation,

$$(U_H+U_{H'})^2 \leqslant (1+U_{H+H'})\,(1+U_{H-H'}), \tag{2}$$

$$(U_H-U_{H'})^2 \leqslant (1-U_{H+H'})\,(1-U_{H-H'}), \tag{3}$$

where U_H stands for U_{hkl}, $U_{H+H'}$ stands for $U_{h+h',\,k+k',\,l+l'}$, etc. These inequalities will yield useful information only when the set of U's under consideration contains a number of coefficients with large values, i.e. values in excess of, say, 0·50. The *h0l* set of reflections, initially investigated by trial and error, was best suited for this requirement. To facilitate using inequalities (2) and (3), the *h0l* set of U's was subdivided into four groups having the property that if two U's are selected from any one group to represent $U_{H+H'}$ and $U_{H-H'}$, then the values of the indices are such that U_H and $U_{H'}$ are present somewhere in the four groups. These four sets of numbers, arranged in decreasing order of magnitude, are listed in Table 1.

To apply inequalities (2) and (3) the terms are chosen so that $|U_{H+H'}| \geqslant |U_{H-H'}|$. Then the following numbers are computed

$$\begin{aligned}(1+|U_{H+H'}|)\,(1+|U_{H-H'}|)&=A,\\ (1+|U_{H+H'}|)\,(1-|U_{H-H'}|)&=B,\\ (1-|U_{H+H'}|)\,(1+|U_{H-H'}|)&=C,\\ (1-|U_{H+H'}|)\,(1-|U_{H-H'}|)&=D,\\ (|U_H|+|U_{H'}|)^2&=E,\end{aligned}$$

and we always have $A \geqslant B \geqslant C \geqslant D$. There are three situations that are of particular interest:

(1) $|U_{H+H'}|>0$, $|U_{H-H'}|>0$, $|U_H|>0$, $|U_{H'}|>0$, $E>B$, C, and D;

conclusion from (1) and (2) is that

$$[U_{H+H'}]=[U_{H-H'}]=[U_H]\,[U_{H'}], \tag{4}$$

where $[U_H]$ is the sign of F_{hkl}, etc.

(2) $|U_{H+H'}|>0$, $|U_H|>0$, $|U_{H'}|>0$, $E>C$ and D;

conclusion: $[U_{H+H'}]=[U_H]\,[U_{H'}]$. (5)

(3) $|U_{H+H'}|>0$, $|U_{H-H'}|>0$, either U_H or $U_{H'}=0$, $E>D$;

conclusion: $[U_{H+H'}]=-[U_{H-H'}]$. (6)

Table 1. *The four independent groups of* U_{h0l} *values for α-selenium*

Modified values are obtained from the relation $U^*_{h0l}=U_{h0l}\exp\,[1{\cdot}4\{(\sin\theta)/\lambda\}^2]$.

Group 1			Group 2			Group 3			Group 4		
H	U_H	U^*_H	H	U_H	U^*_H	H	U_H	U^*_H	H	U_H	U^*_H
$\bar{5}03$	0·65	0·73	507	0·47	0·59	400	0·54	0·58	0,0,10	0·44	0·57
707	0·45	0·62	107	0·46	0·52	206	0·44	0·49	$\bar{2}08$	0·33	0·40
703	0·42	0·53	305	0·39	0·43	2,0,14	0·43	0·73	$\bar{6}08$	0·27	0·37
303	0·41	0·43	309	0·37	0·47	2,0,10	0·41	0·54	$\overline{10}$,0,4	0·23	0·36
$\bar{1}03$	0·35	0·36	1,0,11	0·33	0·46	$\bar{2}02$	0·34	0·35	$\bar{4}06$	0·22	0·26
$\bar{5}07$	0·35	0·44	$\bar{1}09$	0·32	0·40	202	0·33	0·34	$\bar{4}$,0,10	0·22	0·31
307	0·33	0·39	$\bar{1}05$	0·31	0·33	$\bar{2}06$	0·31	0·34	$\bar{2}04$	0·19	0·20
5,0,13	0·33	0·57	709	0·29	0·44	10,0,6	0·31	0·51	006	0·18	0·20
$\bar{1}07$	0·24	0·27	$\bar{3}$,0,11	0·29	0·41	$\bar{6}02$	0·24	0·28	$\bar{8}02$	0·18	0·24
$\bar{3}09$	0·23	0·29	$\bar{3}03$	0·22	0·23	008	0·23	0·27	806	0·15	0·21
$\bar{9}03$	0·23	0·33	503	0·20	0·23	602	0·22	0·26	$\overline{12}$,0,2	0·15	0·27
509	0·22	0·30	705	0·18	0·24	$\bar{8}04$	0·21	0·29	$\bar{2}$,0,12	0·11	0·16
$\bar{3}05$	0·19	0·21	103	0·16	0·16	$\bar{2}$,0,10	0·20	0·26	2,0,12	0·11	0·16
7,0,11	0·17	0·28	$\bar{5}01$	0·16	0·18	004	0·19	0·20	$\bar{8}06$	0·10	0·14
$\bar{1}$,0,11	0·14	0·19	$\bar{5}09$	0·14	0·19	800	0·18	0·23	4,0,10	0·10	0·14
101	0·12	0·12	907	0·12	0·19	808	0·16	0·25	208	0·08	0·10
$\bar{1}$,0,15	0·11	0·20	5,0,11	0·11	0·17	12,0,0	0·15	0·27	608	0·07	0·10
501	0·10	0·11	701	0·08	0·10	804	0·14	0·19	402	0·05	0·05
$\bar{7}05$	0·09	0·12	$\bar{5}05$	0·05	0·06	$\bar{6}06$	0·12	0·15	$\bar{6}04$	0·05	0·06
$\bar{5}$,0,11	0·08	0·12				$\bar{2}$,0,14	0·12	0·20	604	0·05	0·06
$\bar{3}$,0,13	0·08	0·13				$\bar{6}$,0,10	0·11	0·17	0,0,14	0·05	0·08
505	0·07	0·08				408	0·08	0·10			
105	0·03	0·03				$\overline{10}$,0,6	0·08	0·13			
						$\bar{4}04$	0·07	0·08			
						606	0·06	0·08			
						0,0,12	0·05	0·07			
						404	0·04	0·04			

Zero values of U were found for $\bar{3}01$; $\bar{7}01$; 109; 901; 905; $\bar{9}07$; $\bar{7}09$; 3,0,11; 1,0,13; $\overline{11}$,0,1; 11,0,3; $\overline{11}$,0,5; 11,0,7; 909; $\bar{9}$,0,11; $\bar{7}$,0,13 and 3,0,15 in group 1, for $\bar{1}01$; 301; $\bar{3}07$; $\bar{7}03$; $\bar{9}01$; 903; $\bar{9}05$; $\bar{7}07$; $\bar{1}$,0,13; 11,0,1; $\overline{11}$,0,3; 11,0,5; $\overline{11}$,0,7; $\bar{9}09$; $\bar{7}$,0,11; 9,0,11; $\bar{5}$,0,13; 3,0,13; 7,0,13; $\bar{3}$,0,15 and 1,0,15 in group 2, for $\bar{4}08$; $\overline{10}$,0,2; 10,0,2; $\bar{8}08$; 6,0,10; $\bar{4}$,0,12; 4,0,12; $\overline{12}$,0,4; 12,0,4; $\bar{8}$,0,12 and 8,0,12 in group 3 and for 200; 002; $\bar{4}02$; 204; 600; 406; 802; 10,0,0; 10,0,4; 12,0,2; $\overline{10}$,0,8; 10,0,8; $\bar{8}$,0,10; 8,0,10; $\bar{6}$,0,12; 6,0,12; $\bar{4}$,0,14 and 4,0,14 in group 4.

Thus inequalities (2) and (3) will yield the equalities (4), (5) or (6) whenever one of the three situations described is encountered. To discover the combinations of U's that will lead to equalities the data of Table 1 were examined in a systematic way. The strongest U's in the table, all those greater than 0·40 in the present case, are each chosen in turn to represent $U_{H+H'}$ and are paired with every smaller U in their respective groups, including those with zero values, which represent $U_{H-H'}$.

The U's of Table 1 led to 25 equalities from which two signs could be directly determined while 28 signs were expressed in terms of 6 unknown quantities. It was clearly necessary to apply an empirical correction to the U's, as suggested by Gillis, which would artificially increase the magnitude of the coefficients so that the inequalities would yield a practical amount of information. Such a correction is of the form

$$\exp\,[M\{(\sin\theta)/\lambda\}^2],$$

where M is a positive constant which must be chosen by trial and error. There is an upper limit to M set by the fact that none of the U's when multiplied by the correction may exceed unity. In addition, Gillis learned by experience that an excessive value of M would lead to mutually inconsistent derivations of signs. Several values of M were tried and a value of 1·4 was finally selected as the largest which could be used safely without deriving inconsistent results. The set of modified values obtained upon applying this correction are reproduced in Table 1 under the heading U^*_H.

All the U^*'s greater than 0·44 in Table 1 were paired with every smaller U^* in their respective groups, including those with zero values, and inequalities (3) and (4) were applied as before. Group 1 yielded 25 equalities, group 2 led to 30, group 3 to 25, and group 4 to 4.

In addition, the inequality $U^2_H \leqslant \frac{1}{2}(1+U_{2H})$ was used to show that $[2,0,14] = +1$ and $[\overline{10},0,6] = +1$, while the inequality (Gillis, 1948)

$$|\,U_{3H}+3U_H\,| \leqslant 2(1+U_{2H})$$

gave the information that if

$$[800] = -1, \quad \text{then } [400] = -[12,0,0],$$

and that if

$$[\bar{2}06] = -1, \quad \text{then } [\bar{1}03] = -[\bar{3}09].$$

These last two results are useless by themselves and only served to confirm information already obtained from relations (2) and (3).

The net result was to determine 13 signs directly while 42 more signs were expressed in terms of three unknown quantities. Table 2 lists the 55 signs, either directly as positive or negative, or indirectly in terms of the unknown phases b, d and f.

The empirical temperature correction which had been applied to the U's of Table 1 had made it possible to increase greatly the power of the inequalities. At the same time, however, it was on the fringe of being excessive as shown by the fact that six of the 85 equalities obtained with inequalities (2) and (3) were inconsistent with the remaining 79. In addition to this uncertainty the writer had never before used relation (1) for deriving an absolute scale of F values and was concerned about its dependability.

However, when the results were compared with the structure factors which had been calculated earlier by trial and error it was found that there was a surprising correlation between them. When the unknowns b, d and f of Table 2 were all assigned positive values, 33 phases from the two sources were identical.

Refinement by Fourier syntheses

All summations were made with Beevers & Lipson strips and were evaluated at $\frac{1}{60}$ of the cell edges. The initial synthesis on the b-axis projection included only the 33 coefficients whose signs checked with both the phase inequalities and trial-and-error approaches. A second synthesis included 83 coefficients, and the third and final synthesis was made with 88 terms. The doubts expressed about the sign determination by the in-

Table 2. *Phases of α-selenium h0l reflections as derived from the inequalities*

H	U_H	Phase
400	0·58	-1
800	0·23	-1
12,0,0	0·27	$+1$
004	0·20	bd
006	0·20	bdf
008	0·27	$+1$
0,0,10	0·57	$-f$
$\bar{8}02$	0·24	bdf
$\bar{6}02$	0·28	-1
$\bar{2}02$	0·35	$+1$
202	0·34	-1
602	0·26	$+1$
$\bar{9}03$	0·33	$-b$
$\bar{5}03$	0·73	b
$\bar{3}03$	0·23	$-df$*
$\bar{1}03$	0·36	$-b$
103	0·16	df*
303	0·43	$-b$
503	0·23	df
703	0·53	b
$\bar{2}04$	0·20	$-f$
604	0·06	f
$\bar{1}05$	0·33	$-bf$
305	0·43	bf
$\overline{10}$,0,6	0·13	$+1$
$\bar{4}06$	0·26	$-f$
$\bar{2}06$	0·34	-1
206	0·49	$+1$
10,0,6	0·51	-1
$\bar{5}07$	0·44	d
107	0·52	bf
307	0·39	$-d$
507	0·59	$-bf$
707	0·62	d
907	0·19	bf
$\bar{6}08$	0·37	$-f$
$\bar{2}08$	0·40	f
608	0·10	$-f$
$\bar{3}09$	0·29	b
$\bar{1}09$	0·40	bf
309	0·47	$-bf$
509	0·30	d*
709	0·44	bf
$\bar{4}$,0,10	0·31	f
$\bar{2}$,0,10	0·26	$-bd$
2,0,10	0·54	bd
4,0,10	0·14	f
$\bar{3}$,0,11	0·41	bf
1,0,11	0·46	$-bf$
5,0,11	0·17	bf
2,0,12	0·16	f
$\bar{3}$,0,13	0·13	bd
5,0,13	0·57	$-d$
2,0,14	0·73	$+1$
$\bar{1}$,0,15	0·20	d

* Incorrect phases as judged by comparison with final structure.

equalities were unjustified. Of the 55 signs evaluated 52 proved to be correct and the remaining three were related to the six equalities which were inconsistent with the rest of the work. Thus the first synthesis could have included 22 more terms than were used.

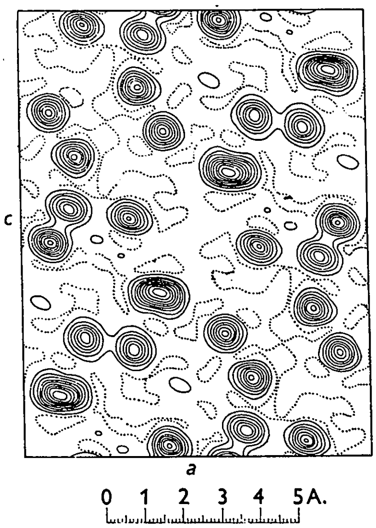

Fig. 1. Electron density of α-selenium projected along the b axis.

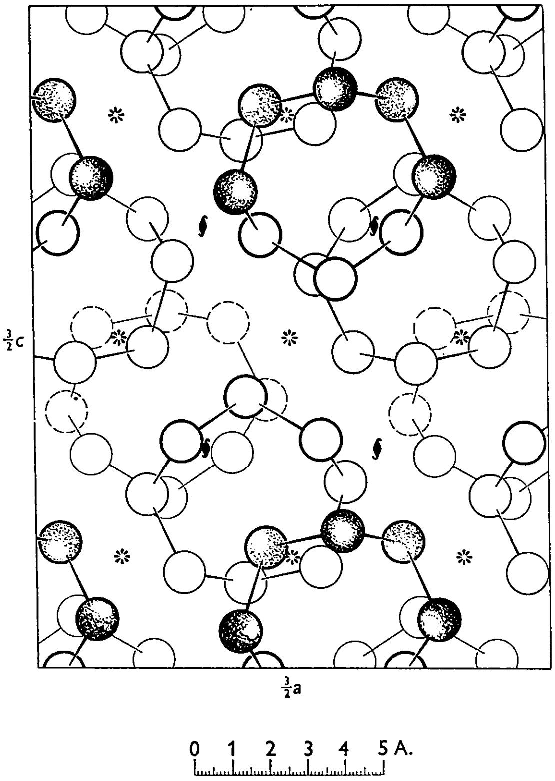

Fig. 2. Crystal structure of α-selenium projected on the (010) plane.

The final electron-density map projected along the b axis is shown in Fig. 1. On this map, and the others which follow, the contours are drawn at equal intervals on a relative scale. The zero level and the positive levels are solid lines while the dotted lines represent negative levels.

Neither the molecular shape nor orientation is at all apparent from a brief inspection of the map. A careful study was made with scale models, assuming a bond distance of 2·34 A. and a bond angle of 105°, but with no assumptions as to molecular shape or the number of atoms in the molecule. After a number of trials it became clear that the atoms were indeed joined into 8-membered ring molecules of the same shape as rhombic sulfur molecules.

In Fig. 2 the structure is shown projected on to the (010) plane. Symmetry centers and screw axes are indicated to show the area of the unit-cell projection since the drawing includes a portion of the contents of all the adjacent unit cells. The molecules are inclined some 20° to the plane of the projection and do not pack together in the manner that rhombic sulfur does.

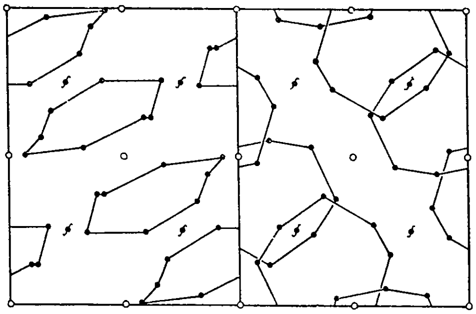

Fig. 3. Comparison of trial-and-error structure (left) with true structure (right).

Fig. 3 compares the x, z co-ordinates deduced by trial and error in the left-hand cell with the final x, z co-ordinates in the right-hand cell. It can be seen that the two sets are qualitatively quite similar. The most interesting feature is that the asymmetric unit derived from the trial-and-error analysis was not a molecule, but consisted of two atoms each from four different molecules. Early conceptions had placed the atoms roughly near three strongly reflecting planes of correctly postulated phase. This had been a sufficient start to deduce the x and z co-ordinates from studies with Bragg & Lipson charts. However, inadequate correlation to molecular models led to completely false ideas on the molecular orientation.

With the molecular shape known, scale molecular models were constructed which enabled the y co-ordinates to be estimated by making the packing radii between molecules approximately equal. The first synthesis of the a-axis projection was made with 37 terms in the series. The fourth and final summation included 86 terms. The electron density projected along the a axis is illustrated in Fig. 4. The molecular resolution is good on this projection and the molecules are seen on edge with their planes roughly normal to the plane of the figure. The atomic resolution is rather poor and only two of the eight atoms in a molecule are completely resolved. The structure is shown projected on to the (100) plane in Fig. 5. The drawing includes a portion of the contents of all the adjacent unit cells.

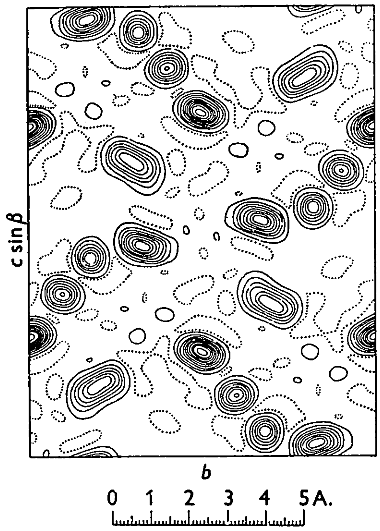

Fig. 4. Electron density of α-selenium projected along the a axis.

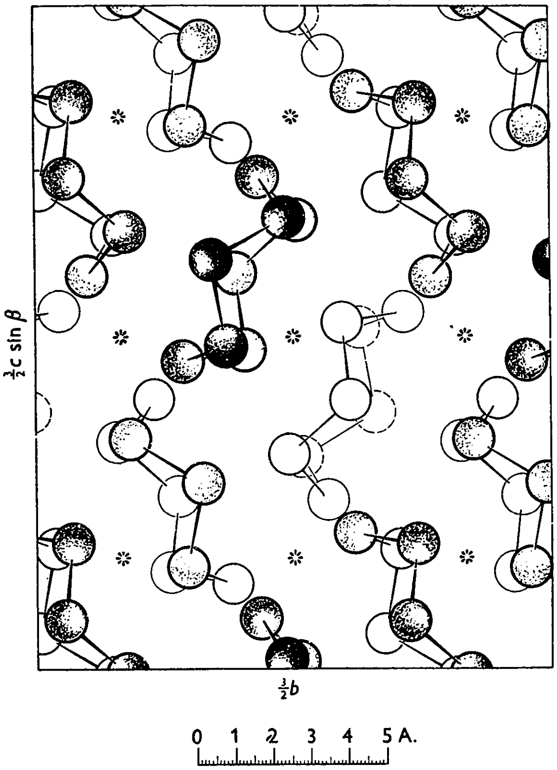

Fig. 5. Crystal structure of α-selenium projected on the (100) plane.

The c-axis synthesis could be made directly and included 85 terms in the summation. Fig. 6 shows the c-axis projection of the electron density. The atomic resolution is most favorable on this projection with all eight atoms clearly separated. This is somewhat surprising since the projected area of the unit cell is smaller than on the other projections. The molecules are also resolved, as shown in Fig. 7 where the structure is projected on to the (001) plane. The molecules are inclined at an angle of some 70° to the plane of the figure.

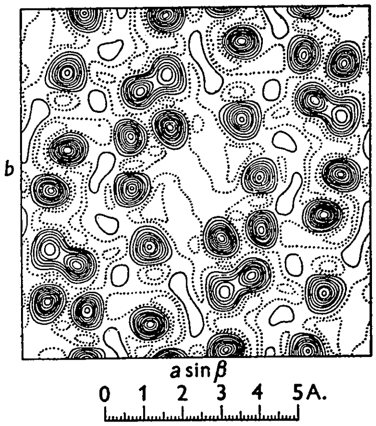

Fig. 6. Electron density of α-selenium projected along the c axis.

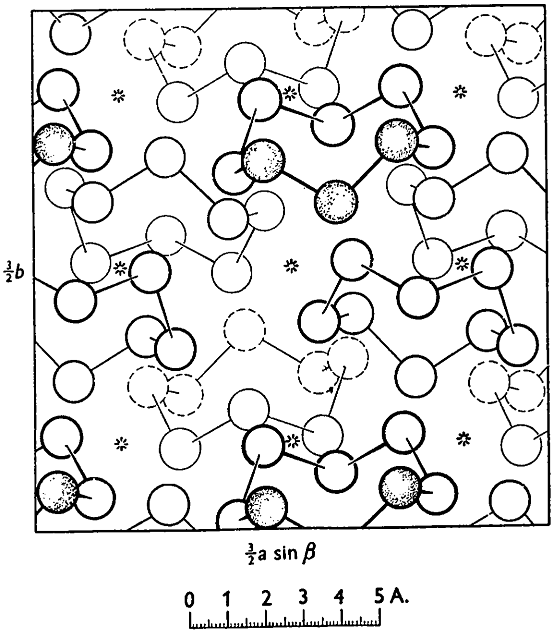

Fig. 7. Crystal structure of α-selenium projected on the (001) plane.

Final parameters and comparison with experiment

All three electron-density projections contributed information for the selection of the final parameters. Only one of the 24 parameters could not be measured from at least one resolved peak. This was the z parameter for atom no. 2 (see Table 3). For the resolved peaks the algebraic method of locating maxima described by Booth (1948) was used, which assumes that the shape of a peak

Table 3. *Parameters determined from the three α-selenium projections*

Atom	x from 88-term $\rho\ (x, z)$	x from 85-term $\rho\ (x, y)$	y from 86-term $\rho\ (y, z)$	y from 85-term $\rho\ (x, y)$	z from 88-term $\rho\ (x, z)$	z from 86-term $\rho\ (y, z)$
1	0·322	0·319	0·484*	0·486	0·237	0·238*
2	0·423*	0·427	0·667*	0·664	0·360*	0·354*
3	0·318	0·316	0·642*	0·637	0·535	0·531*
4	0·136	0·131	0·823	0·818	0·555	0·556
5	−0·081	−0·080	0·696*	0·686	0·521	0·523*
6	−0·157	−0·155	0·740*	0·733	0·328	0·327*
7	−0·085	−0·083	0·520*	0·520	0·229	0·230*
8	0·127*	0·131	0·596	0·597	0·134*	0·134

* Indicates that peak was not resolved.

in the vicinity of a maximum can be represented by a parabola. The estimation of atoms under unresolved peaks was done by graphical means, making use of the shape of the resolved peaks. Table 3 lists the parameters thus determined from the different projections expressed as fractions of the unit-cell edges.

The final parameters were selected from the data of Table 3. When two values were available from resolved peaks an arithmetic mean was taken. When only one value was available from a resolved peak it was used directly. For the z parameter of atom no. 2, the two values from unresolved peaks were averaged to obtain the final value. The list of parameters thus obtained is shown in Table 4.

Table 4. *Final parameters for α-selenium*

Atom	x	y	z
1	0·321	0·486	0·237
2	0·427	0·664	0·357
3	0·317	0·637	0·535
4	0·134	0·820	0·556
5	−0·081	0·686	0·521
6	−0·156	0·733	0·328
7	−0·084	0·520	0·229
8	0·131	0·597	0·134

For the final calculation of structure factors an empirical temperature correction $\exp\left[-B\{(\sin\theta)/\lambda\}^2\right]$ was applied to the atomic scattering factor for selenium with a value of $B=2{\cdot}1\times10^{-16}$ cm.$^{-2}$.

Structure factors were calculated for 367 $h0l$, $0kl$ and $hk0$ reflections.* The correlation function

$$R=(\Sigma\,||F_{\text{obs.}}|-|F_{\text{calc.}}||)/\Sigma\,|F_{\text{obs.}}|$$

has a value of $R=0{\cdot}22$ on the assumption that missing reflections might have been recorded at intensities equal to one-half the minimum observed intensities. If the missing reflections are omitted from the calculation $R=0{\cdot}18$, and, on the other hand, if they are truly zero, then $R=0{\cdot}29$.

Bond lengths and angles

The covalent bond distances are tabulated in Table 5 with a notation such that d_{12} is the covalent bond distance between atom 1 and atom 2. The average value for the Se–Se bond distance is 2·34 ± 0·02 A. (average deviation) which is in exact agreement with the single-bond radius recorded by Pauling (1945). Because all eight covalent bonds in the molecule are identical, it is possible to take an average deviation to estimate the accuracy.

The bond angles are listed in Table 6 with a notation such that α_1 represents the angle subtended at atom 1 by its bonded neighbors.

Table 5. *Covalent bond distances in α-selenium*

$d_{12}=2{\cdot}33$ A.
$d_{23}=2{\cdot}32$ A.
$d_{34}=2{\cdot}36$ A.
$d_{45}=2{\cdot}33$ A.
$d_{56}=2{\cdot}37$ A.
$d_{67}=2{\cdot}34_5$ A.
$d_{78}=2{\cdot}36$ A.
$d_{81}=2{\cdot}31$ A.

Table 6. *Bond angles in α-selenium*

$\alpha_1=107{\cdot}8^\circ$
$\alpha_2=106{\cdot}2^\circ$
$\alpha_3=109{\cdot}0^\circ$
$\alpha_4=101{\cdot}6^\circ$
$\alpha_5=107{\cdot}4^\circ$
$\alpha_6=103{\cdot}9^\circ$
$\alpha_7=102{\cdot}8^\circ$
$\alpha_8=104{\cdot}0^\circ$

The average value for the Se–Se–Se bond angle is 105·3° ± 2·3° (average deviation) which compares with an angle of 105·4° in the rhombic sulfur molecule, and of 105° for metallic selenium. Again an average deviation is taken to assess the accuracy.

Molecular symmetry

It is of interest to know how closely the molecular shape adheres to the idealized non-crystallographic point group symmetry $\bar{8}2m$ which describes the rhombic sulfur molecule. If this symmetry holds, then atoms 1, 3, 5 and 7 will form a square configuration in one plane while atoms 2, 4, 6 and 8 will form a square configuration in another parallel plane.

We can derive the equations of four planes successively using the atoms 1, 3, 5; 3, 5, 7; 5, 7, 1; and 7, 1, 3. These four equations can then be averaged together to give the best plane for all four atoms. If we express the results in orthogonal co-ordinates x', y and z' in Ångström units based on the orthogonal axes a, b and c', with c' perpendicular to the a and b axes, then the equation is

$$x'+8{\cdot}84y-3{\cdot}69z'-31{\cdot}40=0. \qquad (7)$$

The atoms are found to have the following distances from the averaged plane:

Atom	Distance from plane (7)
1	−0·03 A.
3	+0·04 A.
5	−0·05 A.
7	+0·03 A.

---

* Detailed tables of $F_{\text{obs.}}$ and $F_{\text{calc.}}$ are presented in Technical Report XXXVII, Laboratory for Insulation Research, Massachusetts Institute of Technology, June 1950.

The same process for atoms 2, 4, 6 and 8 gives the equation

$$x' + 7{\cdot}00y - 2{\cdot}87z' - 34{\cdot}35 = 0, \tag{8}$$

with the following distances from the averaged plane:

Atom	Distance from plane (8)
2	+0·04 A.
4	−0·04 A.
6	+0·02 A.
8	−0·04 A.

The angle between planes (7) and (8) is found to be equal to 1·9°.

One can see how closely each of these planar arrays approximates to a square array by calculating the angles formed by atoms 1, 3, 5, 7 in one plane, and by atoms 2, 4, 6, 8 in the other plane. Using the notation α_{713} to indicate the angle subtended at atom 1 by atoms 7 and 3, we have the following results:

$$\begin{aligned} \alpha_{713} &= 88{\cdot}4^\circ, & \alpha_{824} &= 89{\cdot}0^\circ, \\ \alpha_{135} &= 91{\cdot}4^\circ, & \alpha_{246} &= 88{\cdot}9^\circ, \\ \alpha_{357} &= 89{\cdot}3^\circ, & \alpha_{468} &= 90{\cdot}5^\circ, \\ \alpha_{571} &= 90{\cdot}9^\circ, & \alpha_{682} &= 91{\cdot}5^\circ. \end{aligned}$$

In plane 1, 3, 5, 7 the average deviation from 90° is $1{\cdot}1_5°$, while in plane 2, 4, 6, 8 the average deviation from 90° is 1·0°.

The molecular configuration can also be expressed in terms of dihedral angles (Pauling, 1949). Using the notation γ_{23} to indicate the dihedral angle formed by the intersection of planes 1, 2, 3 and 2, 3, 4 along the line 2, 3 the following values are obtained:

$$\begin{aligned} \gamma_{12} &= 95{\cdot}8^\circ, & \gamma_{56} &= 103{\cdot}5^\circ, \\ \gamma_{23} &= 101{\cdot}4^\circ, & \gamma_{67} &= 103{\cdot}2^\circ, \\ \gamma_{34} &= 104{\cdot}5^\circ, & \gamma_{78} &= 105{\cdot}8^\circ, \\ \gamma_{45} &= 100{\cdot}0^\circ, & \gamma_{81} &= 101{\cdot}7^\circ. \end{aligned}$$

The average dihedral angle is $102{\cdot}0 \pm 2{\cdot}3^\circ$ (average deviation). The theoretical dihedral angle is calculated from Pauling's expression

$$\sin^2 \tfrac{1}{2}\gamma = \frac{\cos(2\pi/8) + \cos(105{\cdot}3^\circ)}{1 + \cos(105{\cdot}3^\circ)}$$

and gives $\gamma = 101{\cdot}8^\circ$.

The molecular shape does adhere to the symmetry $\bar{8}2m$ within the limits of experimental error.

Intermolecular distances

The notation d_{12} used to represent a bond distance between atoms 1 and 2 of the same molecule is elaborated for representing distances between atoms of different molecules by adding primes to the subscripts as follows:

Subscript unprimed	molecule at x, y, z
Single prime	molecule at $\bar{x}, \bar{y}, \bar{z}$
Double prime	molecule at $\frac{1}{2}+x, \frac{1}{2}-y, \frac{1}{2}+z$
Triple prime	molecule at $\frac{1}{2}-x, \frac{1}{2}+y, \frac{1}{2}-z$.

Thus $d_{4-7''}$ represents the distance between atom 4 on the molecule at x, y, z and atom 7 on the molecule at $\frac{1}{2}+x, \frac{1}{2}-y, \frac{1}{2}+z$.

Since the van der Waals distance of selenium is of the order of 4 A. all intermolecular distances less than 4 A. were sought out and are tabulated in Table 7. The intermolecular distances are believed to be accurate to 0·05 A.

The shorter packing distances, indeed all the distances, are very well arrayed at random in many directions in space. As a result the molecules are bound together quite evenly throughout the three dimensions of the crystal structure. This is in keeping with the properties of α-selenium crystals, for they exhibit no cleavage and tend to develop about equally in all directions in their external habit.

Table 7. *Intermolecular distances in α-selenium*

$d_{4-7''} = 3{\cdot}53$ A.
$d_{6-7'''} = 3{\cdot}57$ A.
$d_{3-6''} = 3{\cdot}61$ A.
$d_{3-5'} = 3{\cdot}64$ A.
$d_{2-7'''} = 3{\cdot}68$ A.
$d_{4-6''} = 3{\cdot}69$ A.
$d_{3-7'} = 3{\cdot}72$ A.
$d_{5-5'} = 3{\cdot}74$ A.
$d_{1-4'''} = 3{\cdot}75$ A.
$d_{2-3'} = 3{\cdot}78$ A.
$d_{5-7'} = 3{\cdot}78$ A.
$d_{1-2'''} = 3{\cdot}84$ A.
$d_{1-8'''} = 3{\cdot}84$ A.
$d_{1-5'} = 3{\cdot}86$ A.
$d_{1-6'''} = 3{\cdot}88$ A.
$d_{3-8''} = 3{\cdot}89$ A.
$d_{3-7''} = 3{\cdot}93$ A.
$d_{1-4''} = 3{\cdot}97$ A.
$d_{2-8'''} = 3{\cdot}98$ A.
$d_{3-6'} = 3{\cdot}98$ A.
$d_{4-8'''} = 3{\cdot}98$ A.
$d_{4-7'} = 3{\cdot}99$ A.

Discussion

The shortest packing distances in Table 7 are of considerable interest, particularly the values 3·53 and 3·57 A. It has generally been assumed that the normal van der Waals distance for selenium is about 4 A. For example, in the structure of thallous thallic selenide (Ketelaar, t'Hart, Moerel & Polder, 1939) each selenium atom has two non-bonded selenium neighbors at 3·84 A. and four more at 4·17 A. On the other hand, there is quite reasonable evidence that the distances observed in metallic selenium are not characteristic of van der Waals forces. There the atoms are in the form of infinite helical chains and are covalently bonded together within the chain. The chains lie parallel to each other in such a fashion that each selenium atom has four neighbors in adjacent chains at a distance of 3·49 A.

To account for the conductivity properties of metallic selenium von Hippel (1948) has interpreted these distances as indicating some metallic character in the bonding, made possible by a resonance between molecular and ionic electron configurations. De Boer (1948) has added further evidence for this line of reasoning. He points out that it is possible to build up a structure of the polyethylene type from planar, zigzag chains in which the number of nearest neighbors belonging to different chains is eight instead of the four in the spiral chain structure. If the valence angles, covalent radii, and van der Waals radii are the same in both structures, then the contribution of the van der Waals forces would determine which is the more stable structure. He concludes that the distance of 3·49 A. in the helical structure is abnormal and could not exist in the zigzag structure. Thus the distance of 3·49 A. is accounted for by metallic forces, and four of these partially metallic bonds have more energy than eight normal van der Waals bonds with a distance of the order of 4 A.

The fact that α-selenium consists of finite ring molecules rather than infinite chains makes it quite obvious why such profound differences exist in the physical properties of α-selenium and metallic selenium. On the other hand, the ring configuration is not a very satisfactory one for selenium as shown by the readiness with which it transforms to the metallic structure on heating.

The writer believes that the shortest packing distances observed in α-selenium are a manifestation of this unstable state of things. They indicate that the atoms involved are being appreciably polarized by atoms in the neighboring molecules. When the ring molecules break open to form chains it is probably these atoms which initiate the process. Also it is clear why the stability of metallic selenium is so high relative to α-selenium. In α-selenium there are at the most only three or four of these shorter intermolecular bonds per eight-atom unit, while in metallic selenium there are 32 intermolecular bonds for every eight atoms.

It is a pleasure to thank Prof. A. von Hippel for suggesting the selenium problem and for providing the writer with the opportunity of carrying out the investigation in the Laboratory for Insulation Research.

References

Boer, F. de (1948). *J. Chem. Phys.* **16**, 1173.

Booth, A. D. (1948). *Fourier Technique in X-ray Organic Structure Analysis.* Cambridge: University Press.

Bradley, A. J. (1924). *Phil. Mag.* **48**, 477.

Buerger, M. J. (1944). *The Photography of the Reciprocal Lattice.* ASXRED Monograph No. 1.

Cochran, W. (1948). *J. Sci. Instrum.* **25**, 253.

Evans, Jr., H. T., Tilden, S. G. & Adams, D. P. (1949). *Rev. Sci. Instrum.* **20**, 155.

Gillis, J. (1948). *Acta Cryst.* **1**, 174.

Halla, F. & Bosch, F. X. (1930). *Z. phys. Chem.* B, **10**, 149.

Harker, D. (1948). *Amer. Min.* **33**, 764.

Harker, D. & Kasper, J. S. (1947). *J. Chem. Phys.* **15**, 882.

Harker, D. & Kasper, J. S. (1948). *Acta Cryst.* **1**, 70.

Hippel, A. R. von (1948). *J. Chem. Phys.* **16**, 372.

Ketelaar, J. A. A., t'Hart, W. H., Moerel, D. & Polder, D. (1939). *Z. Krystallogr.* **101**, 396.

Klug, H. P. (1934). *Z. Krystallogr.* **88**, 128.

Mitscherlich, M. (1856). *Ann. Chim. (Phys.)* **46**, 301.

Muthmann, W. (1890). *Z. Krystallogr.* **17**, 336.

Pauling, L. (1945). *The Nature of the Chemical Bond.* Ithaca: Cornell University Press.

Pauling, L. (1947). *J. Amer. Chem. Soc.* **69**, 542.

Pauling, L. (1949). *Proc. Nat. Acad. Sci., Wash.*, **35**, 495.

Warren, B. E. & Burwell, J. T. (1935). *J. Chem. Phys.* **3**, 6.

Acta Cryst. (1951). **4**, 148

The Crystal Structures of NiO.3BaO, NiO.BaO, $BaNiO_3$ and Intermediate Phases with Composition near $Ba_2Ni_2O_5$; with a Note on NiO

By J. J. Lander

Bell Telephone Laboratories, Inc., Murray Hill, N.J., U.S.A.

(*Received* 12 *May* 1950 *and in revised form* 28 *June* 1950)

The crystal structures of NiO.3BaO, NiO.BaO and $BaNiO_3$ have been determined from X-ray diffraction data, and data are given for phases with composition near that represented by $Ba_2Ni_2O_5$. In each of these structures nickel behaves in a novel fashion. A coplanar triangular arrangement of oxygen around nickel is found in NiO.3BaO. In $BaNiO_3$ nickel has a valence of four and the structure is a close-packed hexagonal stacking of planar arrangements found in perovskite 111 planes. The compound NiO.BaO has a magnetic moment corresponding to two unpaired electrons, whereas the deduced coplanar square arrangement of oxygen around nickel suggests that there should be no unpaired electrons. Compounds with composition near $Ba_2Ni_2O_5$ contain an amount of oxygen which is a continuous function of temperature and possibly contain mixtures of bi- and tetravalent nickel.

The problem of NiO having octahedral co-ordination of oxygen is considered.

Introduction

Current papers (Lander, 1951; Lander & Wooten, 1951) discuss the preparation and properties of barium–nickel oxides. Compounds containing nickel in a valence state higher than two are particularly interesting because relatively little is known about them. A search of the crystallographic literature revealed no studies of such compounds, though there are reports in the chemical literature of mixed oxides in which nickel probably has a valence greater than two. Concerning barium–nickel